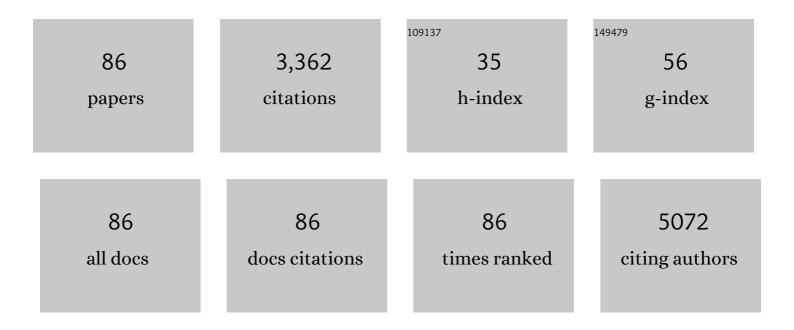
List of Publications by Year in descending order

Source: https://exaly.com/author-pdf/7956723/publications.pdf Version: 2024-02-01



Ιινιιν Ζηλο

#	Article	IF	CITATIONS
1	A Simple Templateâ€Free Strategy to Synthesize Nanoporous Manganese and Nickel Oxides with Narrow Pore Size Distribution, and Their Electrochemical Properties. Advanced Functional Materials, 2008, 18, 1544-1554.	7.8	254
2	Atomic scale insights into structure instability and decomposition pathway of methylammonium lead iodide perovskite. Nature Communications, 2018, 9, 4807.	5.8	161
3	Hierarchical Mesoporous Zeolites: Direct Selfâ€Assembly Synthesis in a Conventional Surfactant Solution by Kinetic Control over the Zeolite Seed Formation. Chemistry - A European Journal, 2011, 17, 14618-14627.	1.7	156
4	Piezoelectric and pyroelectric effects induced by interface polar symmetry. Nature, 2020, 584, 377-381.	13.7	136
5	Suppressing Defectsâ€Induced Nonradiative Recombination for Efficient Perovskite Solar Cells through Green Antisolvent Engineering. Advanced Materials, 2020, 32, e2003965.	11.1	123
6	Mechanisms of electromechanical coupling in strain based scanning probe microscopy. Applied Physics Letters, 2014, 104, .	1.5	121
7	Strain-based scanning probe microscopies for functional materials, biological structures, and electrochemical systems. Journal of Materiomics, 2015, 1, 3-21.	2.8	100
8	Photo-induced ferroelectric switching in perovskite CH <sub>3</sub> NH <sub>3</sub> PbI <sub>3</sub> films. Nanoscale, 2017, 9, 3806-3817.	2.8	86
9	Direct fabrication of mesoporous zeolite with a hollow capsular structure. Chemical Communications, 2009, , 7578.	2.2	84
10	High resolution quantitative piezoresponse force microscopy of BiFeO <sub>3</sub> nanofibers with dramatically enhanced sensitivity. Nanoscale, 2012, 4, 408-413.	2.8	82
11	Templated synthesis of hierarchically porous manganese oxide with a crystalline nanorod framework and its high electrochemical performance. Journal of Materials Chemistry, 2007, 17, 855.	6.7	78
12	Ferroic domains regulate photocurrent in single-crystalline CH3NH3PbI3 films self-grown on FTO/TiO2 substrate. Npj Quantum Materials, 2018, 3, .	1.8	76
13	Mesoporous bioactive glass-coated poly(l-lactic acid) scaffolds: a sustained antibioticdrug release system for bone repairing. Journal of Materials Chemistry, 2011, 21, 1064-1072.	6.7	74
14	Nanoscale Insights into Photovoltaic Hysteresis in Tripleâ€Cation Mixedâ€Halide Perovskite: Resolving the Role of Polarization and Ionic Migration. Advanced Materials, 2019, 31, e1902870.	11.1	73
15	Stabilization of organometal halide perovskite films by SnO2 coating with inactive surface hydroxyl groups on ZnO nanorods. Journal of Power Sources, 2017, 339, 51-60.	4.0	71
16	Strain Engineering of Metal Halide Perovskites on Coupling Anisotropic Behaviors. Advanced Functional Materials, 2021, 31, 2006243.	7.8	71
17	Single crystalline CH3NH3PbI3 self-grown on FTO/TiO2 substrate for high efficiency perovskite solar cells. Science Bulletin, 2017, 62, 1173-1176.	4.3	69
18	Z-scheme Ag3PO4/graphdiyne/g-C3N4 composites: Enhanced photocatalytic O2 generation benefiting from dual roles of graphdiyne. Carbon, 2018, 132, 598-605.	5.4	67

#	Article	IF	CITATIONS
19	Highly flexible, robust, stable and high efficiency perovskite solar cells enabled by van der Waals epitaxy on mica substrate. Nano Energy, 2019, 60, 476-484.	8.2	66
20	Rhodamine B-co-condensed spherical SBA-15 nanoparticles: facile co-condensation synthesis and excellent fluorescence features. Journal of Materials Chemistry, 2009, 19, 3395.	6.7	64
21	Preparation of millimetre-sized mesoporous carbon spheres as an effective bilirubin adsorbent and their blood compatibility. Chemical Communications, 2010, 46, 7127.	2.2	64
22	Delineating local electromigration for nanoscale probing of lithium ion intercalation and extraction by electrochemical strain microscopy. Applied Physics Letters, 2012, 101, 063901.	1.5	54
23	Fabrication of mesoporous zeolite microspheres by a one-pot dual-functional templating approach. Journal of Materials Chemistry, 2009, 19, 7614.	6.7	52
24	CTAB-templated mesoporous TS-1 zeolites as active catalysts in a desulfurization process: the decreased hydrophobicity is more favourable in thiophene oxidation. RSC Advances, 2013, 3, 4193.	1.7	51
25	Epitaxial array of Fe3O4 nanodots for high rate high capacity conversion type lithium ion batteries electrode with long cycling life. Nano Energy, 2020, 74, 104876.	8.2	51
26	Dualâ€Mesoporous ZSMâ€5 Zeolite with Highly <i>b</i> â€Axisâ€Oriented Large Mesopore Channels for the Production of Benzoin Ethyl Ether. Chemistry - A European Journal, 2013, 19, 10017-10023.	1.7	48
27	A micro/mesoporous aluminosilicate: key factors affecting framework crystallization during steam-assisted synthesis and its catalytic property. Journal of Materials Chemistry, 2010, 20, 6764.	6.7	46
28	Switchable Perovskite Photovoltaic Sensors for Bioinspired Adaptive Machine Vision. Advanced Intelligent Systems, 2020, 2, 2000122.	3.3	44
29	Ce-doped SiO2@TiO2 nanocomposite as an effective visible light photocatalyst. Journal of Alloys and Compounds, 2014, 585, 800-804.	2.8	43
30	Touching is believing: interrogating halide perovskite solar cells at the nanoscale via scanning probe microscopy. Npj Quantum Materials, 2017, 2, .	1.8	43
31	Quadratic electromechanical strain in silicon investigated by scanning probe microscopy. Journal of Applied Physics, 2018, 123, .	1.1	42
32	General Decomposition Pathway of Organic–Inorganic Hybrid Perovskites through an Intermediate Superstructure and its Suppression Mechanism. Advanced Materials, 2020, 32, e2001107.	11.1	42
33	Imaging space charge regions in Sm-doped ceria using electrochemical strain microscopy. Applied Physics Letters, 2014, 105, .	1.5	41
34	Environmentally friendly ultrosound synthesis and antibacterial activity of cellulose/Ag/AgCl hybrids. Carbohydrate Polymers, 2014, 99, 166-172.	5.1	40
35	Photocatalytic performances of mesoporous TiO2 films doped with gold clusters. Journal of Materials Chemistry, 2010, 20, 2831.	6.7	36
36	Atomic-scale imaging of CH3NH3PbI3 structure and its decomposition pathway. Nature Communications, 2021, 12, 5516.	5.8	36

#	Article	IF	CITATIONS
37	Transmission electron microscopy of organic-inorganic hybrid perovskites: myths and truths. Science Bulletin, 2020, 65, 1643-1649.	4.3	34
38	Bottom-up tailoring of nonionic surfactant-templated mesoporous silica nanomaterials by a novel composite liquid crystal templating mechanism. Journal of Materials Chemistry, 2009, 19, 6498.	6.7	30
39	Scanning thermo-ionic microscopy for probing local electrochemistry at the nanoscale. Journal of Applied Physics, 2016, 119, .	1.1	28
40	Mapping intrinsic electromechanical responses at the nanoscale via sequential excitation scanning probe microscopy empowered by deep data. National Science Review, 2019, 6, 55-63.	4.6	27
41	P–N depleted bulk BiOBr/α-Fe <sub>2</sub> O <sub>3</sub> heterojunctions applied for unbiased solar water splitting. Dalton Transactions, 2017, 46, 200-206.	1.6	25
42	Metallic tin substitution of organic lead perovskite films for efficient solar cells. Journal of Materials Chemistry A, 2018, 6, 20224-20232.	5.2	24
43	Non-equilibrium microstructure of Li1.4Al0.4Ti1.6(PO4)3 superionic conductor by spark plasma sintering for enhanced ionic conductivity. Nano Energy, 2018, 51, 19-25.	8.2	24
44	Flexible Transparent Highâ€Efficiency Photoelectric Perovskite Resistive Switching Memory. Advanced Functional Materials, 2022, 32, .	7.8	24
45	Hydrothermal epitaxial multiferroic BiFeO3 thick film by addition of the PVA. Journal of Alloys and Compounds, 2013, 577, 44-48.	2.8	21
46	Efficient charge-transport in hybrid lead iodide perovskite solar cells. Dalton Transactions, 2015, 44, 16914-16922.	1.6	20
47	High-efficiency magnetic modulation in Ti/ZnO/Pt resistive random-access memory devices using amorphous zinc oxide film. Applied Surface Science, 2019, 488, 92-97.	3.1	19
48	Polar or nonpolar? That is not the question for perovskite solar cells. National Science Review, 2021, 8, nwab094.	4.6	19
49	Selective doping to relax glassified grain boundaries substantially enhances the ionic conductivity of LiTi2(PO4)3 glass-ceramic electrolytes. Journal of Power Sources, 2020, 449, 227574.	4.0	18
50	Emerging Newâ€Generation Detecting and Sensing of Metal Halide Perovskites. Advanced Electronic Materials, 2022, 8, .	2.6	17
51	A sintering-free, nanocrystalline tin oxide electron selective layer for organometal perovskite solar cells. Science China Materials, 2017, 60, 208-216.	3.5	16
52	Environmentally-friendly sonochemistry synthesis of hybrids from lignocelluloses and silver. Carbohydrate Polymers, 2014, 102, 445-452.	5.1	14
53	Oxygen migration induced effective magnetic and resistive switching boosted by graphene quantum dots. Journal of Alloys and Compounds, 2021, 863, 158339.	2.8	14
54	Preparation of black BiOCl with visible light photocatalytic activity by Fe reduction. Materials Letters, 2014, 116, 98-100.	1.3	13

#	Article	IF	CITATIONS
55	Ultrasonic-Assisted Synthesis of Cellulose/Cu(OH) <sub>2</sub> /CuO Hybrids and Its Thermal Transformation to CuO and Cu/C. Science of Advanced Materials, 2014, 6, 1117-1125.	0.1	13
56	Switchable Perovskite Photovoltaic Sensors for Bioinspired Adaptive Machine Vision. Advanced Intelligent Systems, 2020, 2, 2070092.	3.3	13
57	Ferroic alternation in methylammonium lead triiodide perovskite. EcoMat, 2021, 3, e12131.	6.8	13
58	Resolving fine electromechanical structure of collagen fibrils via sequential excitation piezoresponse force microscopy. Nanotechnology, 2019, 30, 205703.	1.3	12
59	Spatially Resolved Electrochemical Strain of Solid‣tate Electrolytes via High Resolution Sequential Excitation and Its Implication on Grain Boundary Impedance. Small Methods, 2020, 4, 2000308.	4.6	12
60	Trivalent Ni oxidation controlled through regulating lithium content to minimize perovskite interfacial recombination. Rare Metals, 2022, 41, 96-105.	3.6	12
61	Scanning Thermo-Ionic Microscopy: Probing Nanoscale Electrochemistry via Thermal Stress-Induced Oscillation. Microscopy Today, 2017, 25, 12-19.	0.2	11
62	Conduction Response in Highly Flexible Nonvolatile Memory Devices. Advanced Electronic Materials, 2020, 6, 2000151.	2.6	11
63	Electrochemical and oxygen desorption properties of nanostructured ternary compound NaxMnO2 directly templated from mesoporous SBA-15. Microporous and Mesoporous Materials, 2008, 116, 432-438.	2.2	10
64	Preparation and characterization of the continuous titanium-doped ZrO2 mesoporous fibers with large surface area. Journal of Porous Materials, 2014, 21, 105-112.	1.3	10
65	Facile synthesis of CuInGaS2 quantum dot nanoparticles for bilayer-sensitized solar cells. Dalton Transactions, 2014, 43, 16588-16592.	1.6	10
66	Effects of microstructural heterogeneity on fatigue properties of cast aluminum alloys. Journal of Central South University, 2020, 27, 674-697.	1.2	10
67	Competition between activation energy and migration entropy in lithium ion conduction in superionic NASICON-type Li <sub>1â°'3x</sub> Ga <sub>x</sub> Zr <sub>2</sub> (PO <sub>4</sub> ) <sub>3</sub> . Journal of Materials Chemistry A, 2021, 9, 7817-7825.	5.2	10
68	Enhancement in electrochemical catalytic activity of mesoporous RuOxHy and Pt/RuOxHy by gas treatment. Dalton Transactions, 2009, , 3395.	1.6	9
69	The structure, oxygen vacancies and magnetic properties of TiOx (0 < x < 2) synthesized by plasma assisted chemical vapor deposition and reduction. Materials Letters, 2018, 228, 212-215.	1.3	9
70	Tunable engineering of photo- and electro-induced carrier dynamics in perovskite photoelectronic devices. Science China Materials, 2022, 65, 855-875.	3.5	9
71	Enhancing microstructural properties of alumina ceramics via binary sintering aids. Journal of Central South University, 2021, 28, 3705-3713.	1.2	8
72	Role of secondary phase particles in fatigue behavior of high-speed railway gearbox material. International Journal of Fatigue, 2020, 131, 105336.	2.8	7

#	Article	IF	CITATIONS
73	Unraveling atomic-scale lithiation mechanisms in a NiO thin film electrode. Journal of Materials Chemistry A, 2020, 8, 25198-25207.	5.2	7
74	Enhanced photocurrent by the co-sensitization of ZnO with dye and CuInSe nanocrystals. Dalton Transactions, 2015, 44, 12516-12521.	1.6	6
75	Enhanced performance of solar cells via anchoring CuGaS2 quantum dots. Science China Materials, 2017, 60, 829-838.	3.5	6
76	Spatiotemporally Correlated Imaging of Interfacial Defects and Photocurrents in High Efficiency Triple ation Mixedâ€Halide Perovskites. Small, 2022, 18, e2200523.	5.2	5
77	Effect of Clâ^' Concentration on the SCC Behavior of 13Cr Stainless Steel in High-Pressure CO2 Environment. Acta Metallurgica Sinica (English Letters), 2019, 32, 1459-1469.	1.5	4
78	Emerging Intelligent Manufacturing of Metal Halide Perovskites. Advanced Materials Technologies, 2023, 8, .	3.0	3
79	Facile synthesis of superparamagnetic mesoporous zeolite microspheres for the capacious enrichment of enzymes and proteins. Dalton Transactions, 2014, 43, 406-409.	1.6	2
80	Facilely controlling the Förster energy transfer efficiency of dendron encapsulated conjugated organic molecular wire–CdSe quantum dot nanostructures. New Journal of Chemistry, 2015, 39, 1916-1921.	1.4	2
81	Secondary phase induced cracking initiation of high-speed railway gearbox. Materials Science & Engineering A: Structural Materials: Properties, Microstructure and Processing, 2021, 799, 140064.	2.6	2
82	Coupled influence of pore defects on the failure site for high-speed railway gearbox material. Engineering Fracture Mechanics, 2022, 261, 108216.	2.0	2
83	Synthesis and Characteristics of La Doped Ceria–Zirconia Composite with Uniform Nano-Crystallite Dispersion. Science of Advanced Materials, 2010, 2, 43-50.	0.1	1
84	Preface to the special issue on Interdisciplines. Journal of Central South University, 2021, 28, 3639-3641.	1.2	1
85	Forsythia Flower as Natural Photosensitizer for Dye-sensitized Solar Cells. , 2015, , .		0
86	An ultrahigh-voltage 4H-SiC merged PiN Schottky diode with three-dimensional p-type buried layers. Journal of Central South University, 2021, 28, 3694-3704.	1.2	0